

https://doi.org/10.1070/QEL17160

Photosensitivity of composite erbium-doped phosphorosilicate optical fibres to 193-nm laser radiation

A.A. Rybaltovsky, S.A. Vasil'ev, O.V. Butov, O.N. Egorova, S.G. Zhuravlev, S.L. Semjonov, B.I. Galagan, S.E. Sverchkov, B.I. Denker

Abstract. **Results of studying photoinduced changes of a refractive index in the core of a composite erbium-doped phosphorosilicate optical fibre under pulsed UV irradiation at a wavelength of 193 nm and the annealing of these changes are presented and analysed. It is shown that the preliminary saturation of a composite optical fibre by molecular hydrogen substantially increases the photosensitivity. Analysis of thermal anneal kinetics revealed fundamental differences in the photosensitivity mechanisms between the optical fibres saturated with hydrogen and not subjected to hydrogen treatment. Initial and photoinduced absorption spectra of the phosphorosilicate glass are investigated. It is found that in the UV range, the induced absorption is mainly determined by a contribution from the intense absorption band of photoinduced phosphorus electron centres PO_2 with a maximum at 4.7 eV (λ = 260 nm).**

Keywords: *composite optical fibre, phosphate glass, fibre Bragg grating, photosensitivity, induced refractive index, colour centres.*

1. Introduction

Optical fibres doped with rare-earth elements are widely used as active media in fibre lasers and amplifiers of various types. The erbium ion is one of the most important active ions. It has a wide optical gain band in the range of minimal losses of silica fibres (1.55 μm); thus, it is indispensable in telecommunication systems. Fabrication of efficient optical devices often requires a high concentration of erbium ions in the core of the active fibre; however, ion clustering limits increasing the concentration in silica glass. The degree of erbium ion solubility can be increased by the additional doping of silica glass with phosphorous oxide [1]. The limiting concentration of the latter is also limited when glass is produced by standard doping methods such as MCVD. Egorova et al. [2] has demonstrated the possibility of fabricating a composite fibre with SELG (strong erbium laser glass) [3] core and silica cladding in a silica envelope. This new type of a composite fibre provides a possibility to incorporate high-concentration nonclustered erbium ions into the core while keeping compatibility with standard optical-fibre devices, which is necessary for efficient fibre laser systems. An additional important advantage of composite fibres is a substantial photosensitivity (stable change in the refractive index) under irradiation at a wavelength of 193 nm. This provided, for example, creation of a single-frequency erbium fibre laser based on a high-Q Fabry–Perot cavity formed by two fibre Bragg gratings (FBGs) written directly into the fibre [4].

In the present work, photoinduced changes of a refractive index (RI) in the phosphorosilicate composite fibre exposed to radiation of an excimer ArF laser (λ = 193 nm) are more thoroughly studied. The experimental samples were both pristine and H_2-loaded composite optical fibres. Results obtained during the FBG inscription by UV radiation and their thermal annealing performed in the linear heating regime are presented and analysed.

2. Experimental samples and measuring techniques

The tested composite fibre was produced by the technique described in [2]. The chemical composition of the core glass is as follows [4]: 24 mol% P_2O_5/ 3.5 mol% Al_2O_3/2.5 mol% Gd_2O_3/70 mol% SiO_2. The fibre was single-mode in the wavelength range of 1.5 μm (the cut-off wavelength is $\lambda_c \approx 1.4$ μm) and had a step-index profile with a core/cladding difference $\Delta n \approx 0.025$. A diameter of the fibre core was 4.5 μm, the silica cladding diameter was 125 μm.

Spectra of an initial and photoinduced absorption in the UV and visible ranges were recorded by using transverse slices of fibre preform with thicknesses of 0.2 and 0.5 mm. Prior to irradiation, part of the samples with the thickness of 0.2 mm was held for 7 days in an atmosphere of molecular hydrogen at a temperature of 90 °C and pressure of 120 atm. Other fibre samples were saturated at the same temperature and pressure for 24 hours. Absorption spectra were recorded by a PerkinElmer Lambda 900 spectrometer in the range of 190–800 nm.

In this work, an excimer ArF laser (Coherent COMPexPro) with pulses of duration ~20 ns at a pulse repetition rate of 10 Hz was used as a source of UV radiation at a wavelength of 193 nm. Preform slices were subjected to UV radiation through a diaphragm of diameter 1 mm at a pulse energy density of 200 mJ cm^{-2}. FBGs were written in the fibre samples through a phase mask (with the mask period of 1064 nm) at the same energy densities. An FBG in the fibre core was formed due to an interference of ±1 diffraction orders on the phase mask at normal incidence of the UV beam [5]. Uniform (with a constant period along the grating) FBGs with the

A.A. Rybaltovsky, O.V. Butov Kotel'nikov Institute of Radioengineering and Electronics, Russian Academy of Sciences, ul. Mokhovaya 11, korpus 7, 125009 Moscow, Russia; e-mail: rybaltovsky@yandex.ru;
S.A. Vasil'ev, S.G. Zhuravlev, S.L. Semjonov Fiber Optics Research Center, Russian Academy of Sciences, ul. Vavilova 38, 119333 Moscow, Russia;
O.N. Egorova, B.I. Galagan, S.E. Sverchkov, B.I. Denker Prokhorov General Physics Institute, Russian Academy of Sciences, ul. Vavilova 38, 119333 Moscow, Russia

Received 15 October 2019
Kvantovaya Elektronika **49** (12) 1132–1136 (2019)
Translated by N.A. Raspopov

length of 3–10 mm and the reflection coefficient $R \approx 99\%$ were recorded and investigated.

FBG annealing was performed in a resistive oven in the regime of linear heating at three rates dT/dt differing pairwise by 5 times: 0.05, 0.25, 1.25 K s^{-1} [6,7]. In the process of FBG writing and annealing, transmission spectra of the grating were measured by an optical Yokogawa AQ6370D spectrum analyser at the maximal spectral resolution of 0.02 nm.

A modulation amplitude of the induced refractive index (induced RI) Δn_{mod} was calculated from the measured FBG reflection coefficient, and the average value of Δn_{avr} was found from the shift of the resonance wavelength λ_{res} by known formulae presented, for example, in [8].

3. Experimental results

3.1. Initial and photoinduced absorption

The initial absorption spectrum of a core glass measured in a transverse slice of an optical fibre preform is shown in Fig. 1a. Absorption bands of Er^{3+} ions are well distinguished in the visible range [9], as well as the UV bands of Gd^{3+} ion absorption with the maxima at 4.3, 5.1, 5.5, and 6 eV, which correspond to intraconfigurational 4f–4f transitions [10].

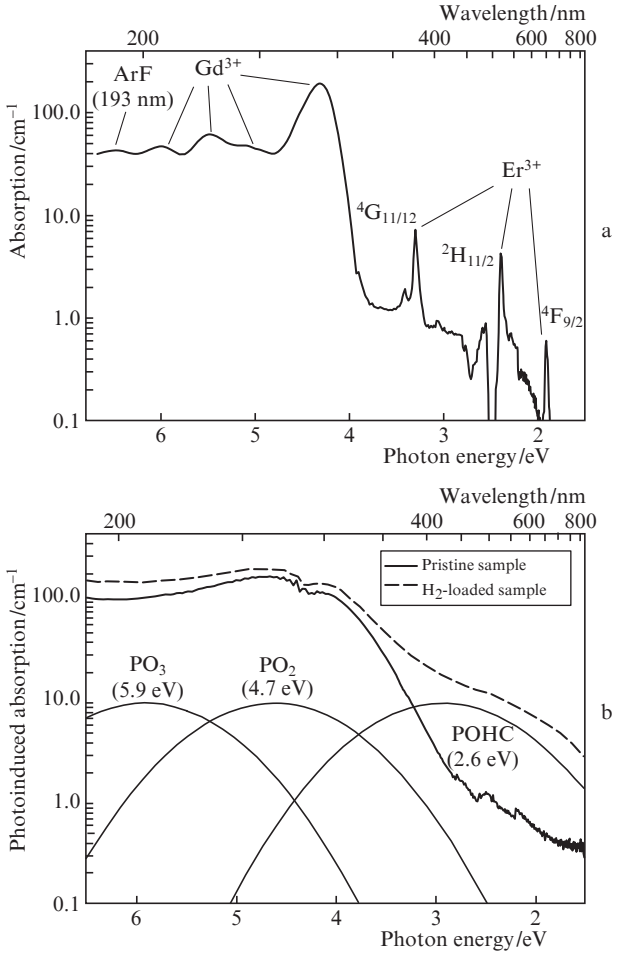

Figure 1. Spectra of (a) an initial and (b) photoinduced absorption of a phosphate core glass.

The absorption coefficient at the irradiation wavelength of 193 nm is ~ 40 cm^{-1}. If we assume that the absorption spectrum does not noticeably change in the process of fibre drawing, then part of absorbed radiation in the optical fibre core is relatively small ($\sim 2\%$). Within the accuracy of our measurements, the absorption spectrum of bulk samples did not change after the hydrogen treatment.

According to conclusions in [11], absorption at $\lambda = 193$ nm in pure phosphorosilicate glass is mainly related to the band of phosphorous oxygen-deficient centres (PODCs) with a maximum at 6.9 eV. We may assume that in the tested samples, at the irradiation wavelength of 193 nm, the absorption of Gd^{3+} ions is added to the PODC absorption mentioned above. Weak bands of Er^{3+} ions do not substantially affect the absorption value near 193 nm.

As follows from the parameters of the tested fibre, phosphorous oxide has the highest concentration (24 mol%) among other dopants. According to papers [12–15], when UV, X-ray, or gamma radiation affect a phosphate glass lattice, colour centres are formed with the absorption bands located mainly in the visible and UV spectral ranges [16,17]. Let us analyse spectra of induced absorption in the preform slices irradiated by a dose $D_{UV} = 1.2$ kJ cm^{-2} (Fig. 1b). One can see that the induced absorption in the wavelength range of 200–800 nm is mainly due to the band with a maximum at 4.7 eV (260 nm), which is ascribed to the absorption of electron centres PO_2 [14]. In the hydrogenated sample, the structure of these centres is modified by atomic hydrogen HPO_2 [15]. In addition to the absorption band at 4.7 eV, the shape of spectra presented in Fig. 1b in the range of 5.5–6.5 eV can be explained by a contribution of the sufficiently intensive shorter-wavelength band with a maximum near 6.6 eV, which, seemingly, is related to absorption by oxygen-deficient centres [16]. In the visible part of the spectrum of the hydrogenated sample (dashed curve) one can see a contribution from the low-intensity band with a maximum near 2.5 eV, which can be ascribed to absorption by defects of the type 'self-trapped holes' [17]. On the whole, taking into account the contribution from the bands at 2.5, 4.7, and 6.6 eV, it is possible to describe the shape of the induced absorption spectrum both in pristine and hydrogenated samples.

Note that the induced absorption is substantial (at the maximum: 180 cm^{-1} (pristine) and 220 cm^{-1} (hydrogenated), which, as follows from Fig. 1, is several times greater than the initial absorption in the range 4.5–6.5 eV); hence, according to the Kramers–Kronig relations, it may noticeably contribute into the induced index value at a wavelength of ~ 1.5 μm [18,19]. Note in additionthat absorption at the radiation wavelength of the excimer laser, i.e. at 193 nm, also noticeably increases under UV irradiation, which should enlarge the fraction of the power absorbed in the composite fibre core in the process of FBG writing.

3.2. UV-induced refractive index change

The dependences of the modulation amplitude Δn_{mod} and the average induced RI Δn_{avr} on the irradiation dose, measured for pristine and hydrogenated fibres are shown in Fig. 2 in double logarithmic scales. In both the cases, the UV radiation at a wavelength of 193 nm results in a positive contribution into the RI, which, similarly to many other photosensitive glass compositions, is well described by a power function of dose $\Delta n \sim D^b$. In this case, the power is $b = 0.58 \pm 0.02$ for the pris-

tine fibre and $b = 0.85 \pm 0.02$ for the H_2-loaded one. Similarly to Ge-doped optical fibres, molecular hydrogen in the composite fibre core substantially (at least by 5 times) increases the photosensitivity.

Note that the induced RI dependences on dose presented in Fig. 2 substantially differ from those measured with the phosphorosilicate fibres produced by the MCVD method, which exhibit a close-to-quadratic dependence at the initial part [20, 21].

Photosensitivity of phosphate glass fibres under irradiation at a wavelength of 193 nm was studied in [22, 23]. Results of these works mainly differ from our results both in FBG writing and in their thermal annealing. Seemingly, this is explained by different core glass compositions and by the cladding with a low thermal expansion coefficient (TECF), which introduces distinctive features to the considered processes.

Dependences obtained for the pristine fibre show (Fig. 2) that a contrast of the induced RI in the FBG structure (the ratio $\Delta n_{mod}/\Delta n_{avr}$) is 0.7–0.8 with our inscription technique. However, at high radiation doses ($D_{UV} > 500$ J cm^{-2}) the induced RI contrast in the H_2-loaded fibre substantially falls due to a noticeable saturation of the modulation amplitude. As a rule, in such cases it is assumed that the fall in the FBG structure contrast occurs due to inhomogeneous illumination (mechanical instability of a recording system, etc.) and/or nonlinearity in the dose dependence, which results in the induced RI saturation in the intensity maximum and leads to higher spatial harmonics. However, a comparison with the growing of Δn_{mod} in the pristine fibre shows that the influence of these two factors is not confirmed. The contrast of the FBG structure does not fall or falls insignificantly at the radiation doses up to 2 kJ cm^{-2}, and the linearity of the dose dependence in the hydrogenated fibre is even higher than in the pristine one.

The fall of the FBG structure contrast for the H_2-loaded fibre may be explained as follows. Due to a large difference in the TECs of core and cladding, the composite fibre core at room temperature is subjected to substantial tensile stresses, which slightly reduce the core RI due to the elasto-optic effect. The UV irradiation of the hydrogenated glass causes restructuring of the glass network accompanied with the breaking of regular and defect bonds with the subsequent saturation of those by hydrogen atoms, which results in origin of hydride and hydroxyl groups [24]. At tensile stresses, this process may dilute the glass network in the irradiated core parts and compact it in unirradiated ones. Thus, we may assume that an additional index grating arises, which is related with the change in the glass core density mentioned above; the RI change for this grating has the opposite sign relative to that of the main FBG. A consequence of this process is a fall in the modulation amplitude of the induced RI. Note that relaxation of tensile stresses in the composite fibre core should also lead to an additional increase in the core average induced RI.

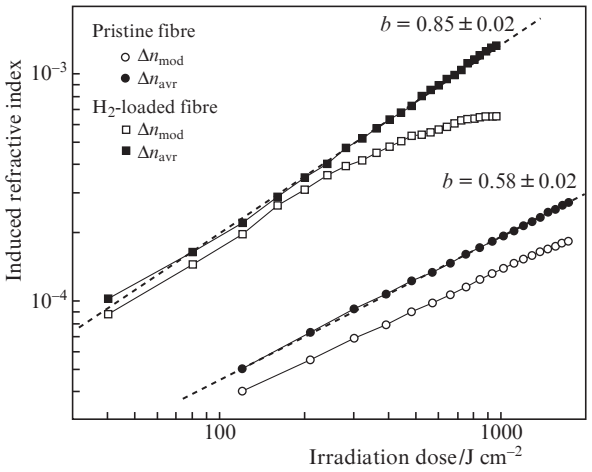

Figure 2. Dependences of the modulation amplitude (○,□) and an average value (●,■) of induced RI on the UV irradiation dose for pristine and H_2-loaded fibres.

3.3. Annealing the photoinduced refractive index

Results of annealing the FBG written in the pristine fibre are presented in Fig. 3. In Fig. 3a, a relative change in the modulation amplitude of the induced RI is shown (normalised to the initial value measured at $T \approx 300$ K) versus the oven temperature. The data presented have been obtained by annealing three FBGs at different constant heating rates. One can see that in all the cases, Δn_{mod} monotonically reduces as the oven temperature increases up to the softening temperature of the composite fibre core material (900–1000 K) [3]; the slower heating is, the earlier (at lower temperatures) the FBG is annealed. The dependences presented make it possible to

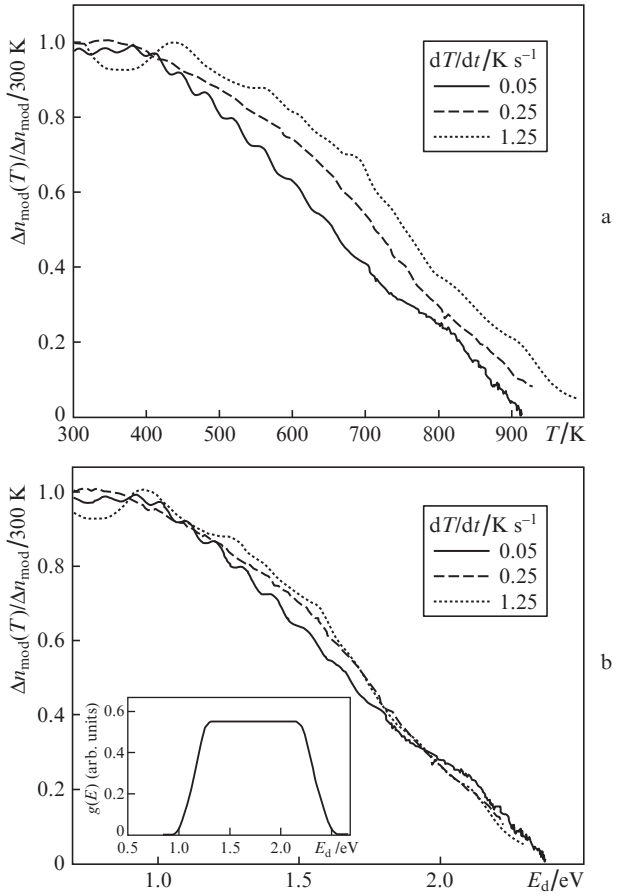

Figure 3. (a) Annealing dependences of the normalised value Δn_{mod} of FBG, measured at three heating rates and written to the pristine fibre. (b) Similar dependences in the coordinates of demarcation energy E_d in the case of the best superposition.

plot the so-called base curve [25] for a temperature resistance of the induced RI in the fibre, which allows one to calculate changes of FBG properties in a more general case of an arbitrary-type heat exposure including a long-term FBG operation. For plotting the master curve, dependences obtained experimentally are juxtaposed in the demarcation energy coordinates $E_d = kT\ln(v_0 t)$, where k is the Boltzmann constant; T is the absolute temperature; $v_0 = 10^n$ is the frequency factor; and t is the time [25]. The juxtaposition is realised by fitting the frequency factor, namely, power n. Note that conventionally random and systematic measurement errors prevent accurate juxtaposition of the dependences in the whole range of Δn_{mod} variation; hence, the accuracy of the frequency factor determination is not high. In our case, the accuracy was within two orders: $v_0 \approx 10^{9\pm2}$ Hz.

Juxtaposition of the measured dependences in E_d coordinates obtained at $n = 9$ is shown in Fig. 3b. One can see that the master curve in this case is actually a straight line; hence, its derivative $g(E)$ shown schematically in the inset of Fig. 3b looks like a trapezium with a flat top of length ~1 eV. Conventionally, it is assumed that induced RI annealing brings the glass network to the initial state, that is, network modifications induced by the UV radiation are thermally reversible. Here, the function $g(E)$ is considered as a distribution of activation barriers of thermo-induced reverse transitions. Thus, under the assumption that the induced RI in the pristine fibres irradiated at a wavelength of 193 nm is formed due to a single photoinduced process (mechanism), the dependences in Fig. 3 make us assume that network variations substantially depend on a local environment (are substantially inhomogeneous). In the network of SELG activated by rare-earth ions, sites with the highest nonuniformity are mainly localised near rare-earth ions (in the present work near erbium and gadolinium ions), because atoms of phosphorus, aluminium, and oxygen may simultaneously be located within the first coordination sphere of a single ion [26]. In view of a substantial contribution of Gd^{3+} ion absorption to the initial absorption at a wavelength of 193 nm, it is reasonable to assume that the UV-induced transformations of a glass lattice and generation of colour centres mainly occur in the nearest environment of gadolinium atoms.

Similar dependences measured with FBGs written in the H_2-loaded fibres are presented in Fig. 4. These are more complicated, namely: at a temperature of 600 K, the fall in the modulation amplitude stops and then continues again through ~100 K. The best juxtaposition of the dependences recorded at different heating rates (Fig. 4a) is realised at the frequency factor $v_0 \approx 10^9$ Hz. Similarly to the previous case, due to the relatively small difference in the heating rates (25 times) the error of determining this value is no better than two orders of magnitude (Fig. 4b).

A derivative of the base curve, obtained for this case is presented in the inset of Fig. 4b. A 'double-peak' shape of the dependence allows one to assume two mechanisms, which make comparable contributions into the induced RI and have different temperature resistance. We may also assume that the mechanism of the induced RI formation in hydrogenated fibres is similar to that in pristine fibres, and the plane part of the anneal curves, which entails the dip in the central part of function $g(E)$, is related to annealing the density grating with the opposite induced RI sign discussed above.

One more controlled parameter in our experiments on annealing FBGs was the change of the resonance wavelength λ_{res}, which, in a general case, comprises reversible and irreversible components [27]. The irreversible part of λ_{res} variation characterises the annealing of the average induced RI and, as a rule, is substantially less than the reversible part, which in optical fibres on silica glass is related to a thermo-optic coefficient dn/dT [28].

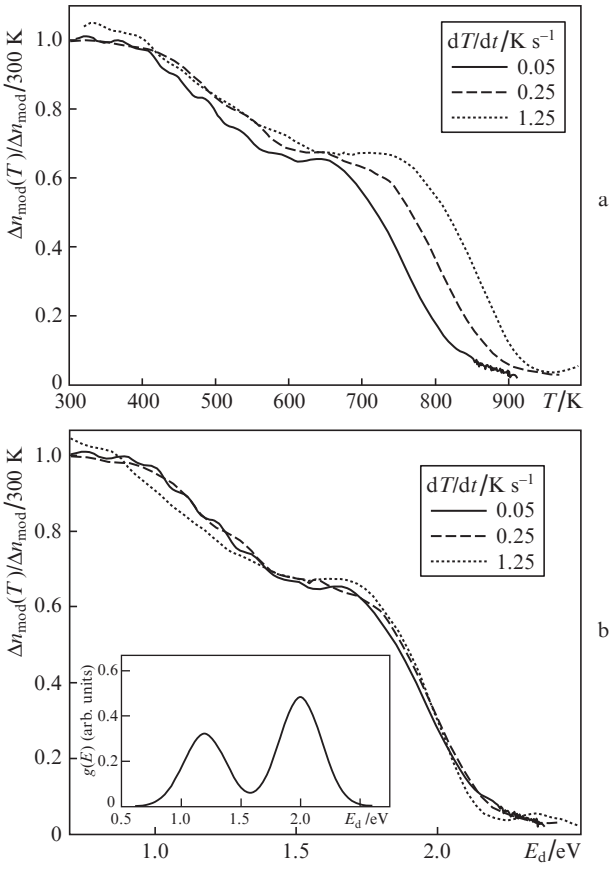

Figure 4. (a) Annealing dependences of a normalised value Δn_{mod} of FBG, measured at three heating rates and written in the H_2-loaded fibre. (b) Similar dependences in the coordinates of demarcation energy E_d in the case of the best superposition.

A temperature sensitivity of FBGs (the reversible change of λ_{res}) written both in pristine and H_2-loaded fibres is ~ 9.3 pm K^{-1} (~ 6.0 ppm K^{-1}) in the range 25–100 °C, which is a little less than the value, typical for FBGs recorded in germanium-silicate optical fibres ~10.3 pm K^{-1} (~ 6.6 ppm K^{-1}). The difference may relate to a lower thermo-optic coefficient of the composite core glass [3], and by thermo-induced changes of mechanical stresses in the central part of a composite optical fibre, which result in RI changes due to the elasto-optic effect.

4. Conclusions

A high photosensitivity of composite erbium-doped fibre to pulsed laser radiation at a wavelength of 193 nm is demonstrated. It was established that the preliminary saturation of the optical fibre by molecular hydrogen at a temperature of 90 °C and pressure of 120 atm increases the photosensitivity by approximately 5 times. In the irradiated samples of composite fibre preforms, a substantial (by more than 100 cm^{-1}) increase in the UV absorption was found, which is mainly related to the absorption band near 4.7 eV (260 nm) of PO_2 electron centres. In preliminarily hydrogen-loaded samples,

it is related to HPO_2 centres modified by hydrogen. The induced RI dependences on the irradiation dose are well described by the power function $\Delta n \sim D^b$.

Experiments on the linear temperature annealing of photoinduced FBGs were performed. In the result, kinetics of an induced RI temperature decay was obtained both in pristine and H_2-loaded composite fibre samples. It was shown that in the irradiated pristine samples, kinetics of temperature decay is monotonically falling up to the core–glass softening temperature of 900–1000 K. On the contrary, kinetics of the induced RI decay in H_2-loaded samples exhibits stability in the range of 600–700 K. This can be explained both by an influence of two mechanisms of forming the induced RI with different temperature stabilities, and by annealing of the opposite-sign RI grating, which is related to redistribution of the core material density.

Acknowledgements. The work was performed in the frameworks of a state assignment.

References

1. Jiang S., Luo T., Hwang B.C., Smekatala F., Seneschal K., Lucas J., Peyghambarian N. *J. Non-Cryst. Solids*, **263**, 364 (2000).
2. Egorova O.N., Semjonov S.L., Velmiskin V.V., Yatsenko Yu.P., Sverchkov S.E., Galagan B.I., Denker B.I., Dianov E.M. *Opt. Express*, **22**, 7632 (2014).
3. Karlsson G., Laurell F., Tellefsen J., Denker B., Galagan B., Osiko V., Sverchkov S. *Appl. Phys. B*, **75**, 41 (2002).
4. Rybaltovsky A.A., Egorova O.N., Zhuravlev S.G., Galagan B.I., Sverchkov S.E., Denker B.I., Semjonov S.L. *Opt. Lett.*, **44** (14), 3518 (2019).
5. Vasil'ev S.A., Medvedkov O.I., Korolev I.G., Bozhkov A.S., Kurkov A.S., Dianov E.M. *Quantum Electron.*, **35** (12), 1085 (2005) [*Kvantovaya Elektron.*, **35** (12), 1085 (2005)].
6. Rathje J., Kristensen M., Pedersen J.E. *J. Appl. Phys.*, **88** (2), 1050 (2000).
7. Bozhkov A.S., Vasil'ev S.A., Medvedkov O.I., Grekov M.V., Korolev I.G. *Instrum. Exp. Tech.*, **48** (4), 491 (2005) [*Prib. Tekh. Eksp.*, (5), 76 (2005)].
8. Medvedkov O.I., Vasiliev S.A., Gnusin P.I., Dianov E.M. *Opt. Mater. Express*, **2** (11), 1478 (2012).
9. Wang F., Song F., An S., Wan W., Guo H., Liu S., Tian J. *Appl. Opt.*, **54** (5), 1198 (2015).
10. Wang Y., He J., Barua P., Chiodini N., Steigenberger S., Abdul-Khudus M.I.M., Sahu J.K., Beresna M., Brambilla G. *APL Photon.*, **22**, 046101 (2017).
11. Rybaltovsky A.A., Sokolov V.O., Plotnichenko V.G., Lanin A.V., Semenov S.L., Gur'yanov A.N., Khopin V.F., Dianov E.M. *Quantum Electron.*, **37** (4), 388 (2007) [*Kvantovaya Elektron.*, **37** (4), 388 (2007)].
12. Ehrt D., Ebeling P., Natura U. *J. Non-Cryst. Solids*, **263**, 240 (2000).
13. Ebeling P., Ehrt D., Friedrich M. *Opt. Mater.*, **20** (2), 101 (2002).
14. Griscom D.L., Friebele E.J., Long K.J., Fleming J.W. *J. Appl. Phys.*, **54** (7), 3743 (1983).
15. Hosono H., Kajihara K., Hirano M., Oto M. *J. Appl. Phys.*, **91** (7), 4121 (2002).
16. Girard S., Kuhnhenn J., Gusarov A., Brichard B., Van Uffelen M., Ouerdane Y., Boukenter A., Marcandella C. *IEEE Transact. Nucl. Sci.*, **60** (3), 2015 (2013).
17. Sasajima Y., Tanimura K. *Phys. Rev. B*, **68**, 014204 (2003).
18. Kitamura R., Pilon L., Jonasz M. *Appl. Opt.*, **46** (33), 8118 (2007).
19. Leconte B., Xie W.X., Douay M., Bernage P., Niay P., Bayon J.F., Poignant H. *Appl. Opt.*, **36** (24), 5923 (1997).
20. Strasser T.A., in *Optical Fiber Communication Conf.* (OFC-96) (San Jose, USA) TuO1.
21. Larionov Yu.V., Rybaltovsky A.A., Semenov S.L., Kurzanov M.A., Obidin A.Z., Vartapetov S.K. *Quantum Electron.*, **33** (10), 919 (2003) [*Kvantovaya Elektron.*, **33** (10), 919 (2003)].
22. Xiong L., Hofmann P., Schülzgen A., Peyghambarian N., Albert J. *Opt. Mater. Express*, **4** (7), 1427 (2014).
23. Albert J., Schülzgen A., Temyanko V.L., Honkanen S., Peyghambarian N. *Appl. Phys. Lett.*, **89** (10), 101127 (2006).
24. Lancry M., Poumellec B., Niay P., Douay M., Cordier P., Depecker C. *J. Non-Cryst. Solids*, **351** (52–54), 3773 (2005).
25. Erdogan T. *J. Lightwave Technol.*, **15** (8), 1277 (1997).
26. Funabiki F., Kamiya T., Hosono H. *J. Ceram. Soc. Jpn*, **120** (11), 447 (2012).
27. Gnusin P.I., Vasil'ev S.A., Medvedkov O.I., Dianov E.M. *Quantum Electron.*, **40** (10), 879 (2010) [*Kvantovaya Elektron.*, **40** (10), 879 (2010)].
28. Kersey A.D., Davis M.A., Patrick H.J., LeBlanc M., Koo K.P., Askins C.G., Friebele E.J. *J. Lightwave Technol.*, **15** (8), 1442 (1997).